Investigation of perched water generation mechanisms through full-scale embankment model tests

Katsuyuki Kawai*,[1], Satsuki Kataoka[2], and Haruto Tomochika[3]

[1]*Department of Civil and Environmental Engineering, Kindai University, Higashi-Osaka, Japan*
[2]*School of Regional Innovation and Social design Engineering, Kitami Institute of Technology, Kitami, Japan*
[3]*Land Infrastructure Department, Pacific Consultants, Sapporo, Japan*
**Corresponding author's email:* kkawai@civileng.kindai.ac.jp

Abstract: When constructing earth structures such as road embankments, bottom drainage structures are generally provided to drain infiltrated rainwater. However, in some cases, surface failure occurs mid-slope before encountering the drainage structures. This phenomenon arises from the generation of "perched water," which has a phreatic surface independent of the groundwater level at the bottom of embankment and occurs when localized low permeability areas within the embankment accumulate water above them. To investigate construction methods to prevent perched water generation and to develop methods to eliminate perched water in existing structures, it is important to understand the mechanisms of perched water development. In this study, full-scale embankment model tests were conducted to capture the generation and dissipation behavior of perched water within earth structures. Tensiometers and soil moisture meters were installed for monitoring, and electrical prospecting was periodically conducted. Consequently, perched water generation was found dependent on both rainfall pattern and the permeability gap between soil layers, while perched water dissipated easily on low permeability layers with an incline.

Introduction

With the scaling up of construction machinery, the construction of high embankments has become possible. The rise of the phreatic surface within the embankment significantly impacts its stability, and the importance of drainage structures increases with embankment size to reduce the risk of embankment failure. When designing embankments, the embankment material is often assumed to be homogeneous. In these cases, the highest risk for failure is considered to occur when the phreatic surface forms at the base of the embankment, with the embankment toe becoming the tip of the failure mass. However, due to the heterogeneity of embankment materials and the variability in construction quality even in uniform materials, low permeability layers may form locally within the embankment. These layers may result in the formation of perched water, a free water layer independent of the phreatic surface at the

base of the embankment (Photo 1). The development of perched water can lead to shallow failures not anticipated during the design process. Fukada et al. [1] have indicated that perched water forms in boundary layers with permeability differences on the order of 100 times. This study aims to clarify the mechanisms of formation and dissipation of perched water by constructing a layered experimental embankment that satisfies the conditions for perched water formation and then monitoring the process of perched water development under rainfall.

Overview of the embankment model and the experimental procedure

Two types of construction waste soil, Soil A and Soil B with particle grading curves as shown in Figure 1, were prepared for constructing the embankment model. Soil A has a higher proportion of fine particles, and a distinct compaction curve as obtained from the compaction test (Figure 2). Figure 3 shows the results of the permeability test conducted on the compacted specimens (JIS A 1218), where permeability was found to depend on degree of compaction, Dc. In previous studies, numerical simulation found that perched water tends to form above layers where the permeability coefficient is reduced by more than one-hundredth. Based on the relationship between the degree of compaction and permeability coefficient, as shown in Figure 3, compaction control values were determined for constructing the embankment model. An

Photo 1: Leachate of perched water from berm of embankment

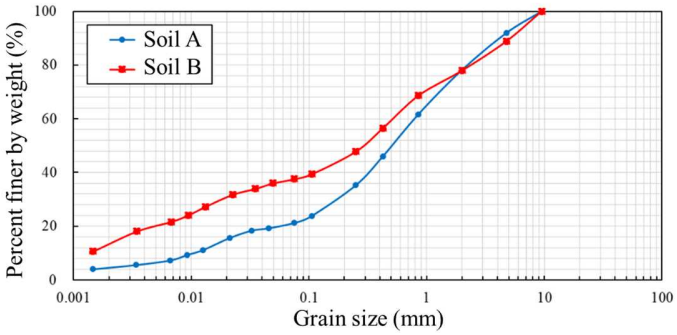

Figure 1: Particle gradation curves

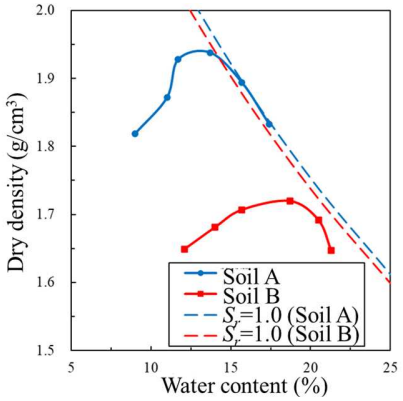

Figure 2: Compaction curves

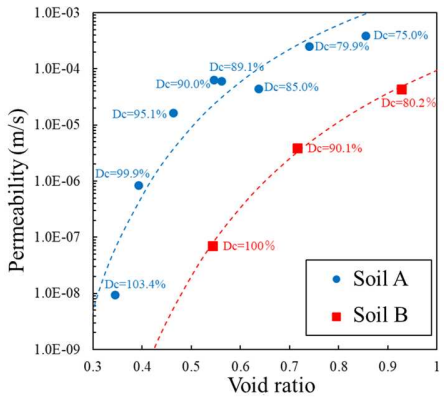

Figure 3: Permeability of compacted soil

Photo 2: Embankment model

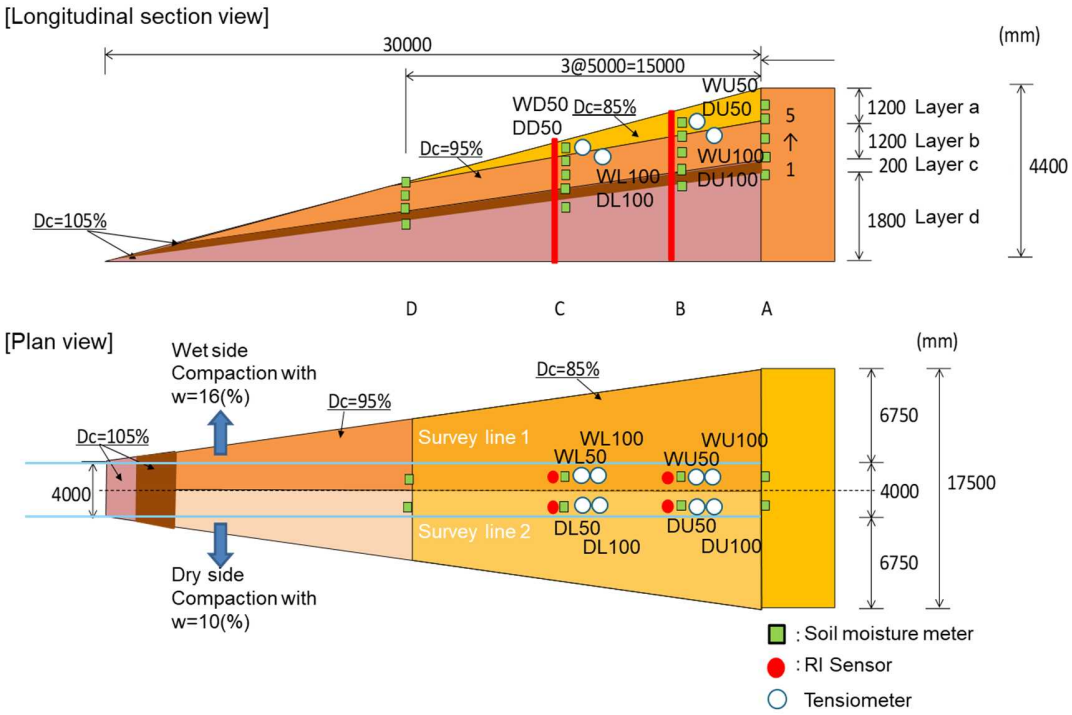

Figure 4: Schematic diagram of the embankment

embankment with a crest width of 4 m, a height of 4.4 m, and a horizontal slope length of 30 meters was constructed at Kobe Airport Island in 2022, as shown in Photo 2 and Figure 4. The embankment consisted of four layers: Layer d, made of cement-stabilized Soil A as an impermeable subgrade; Layer c, constructed with Soil B compacted to 105% (compacted to more than the maximum dry density) to form a perched water aquifer; Layer b, consisting of Soil A compacted to 95%; and Layer a, constructed with Soil A compacted to 85%. It was assumed that perched water would form above Layers b and c. Layer b was divided into two sections: a Dry side to the west, constructed at 10% of the optimum water content, and a Wet side to the east, constructed at 6% more than the optimum water content. A total of 38 soil moisture sensors were installed in Layers a and b, with a wireless tensiometer placed at depths of 50 and 100 cm from the slope surface, as shown in Figure 4. The symbols in Figure 4 indicate the location of the tensiometer. For example, WD100 refers to the tensiometer located at a depth of 100 cm on Lower part of the Wet side. Electrical prospecting on Survey lines 1 and 2, expressed by light blue lines, was periodically conducted throughout the observation period, using a dipole-dipole electrode configuration. Along the longitudinal section, electrodes for

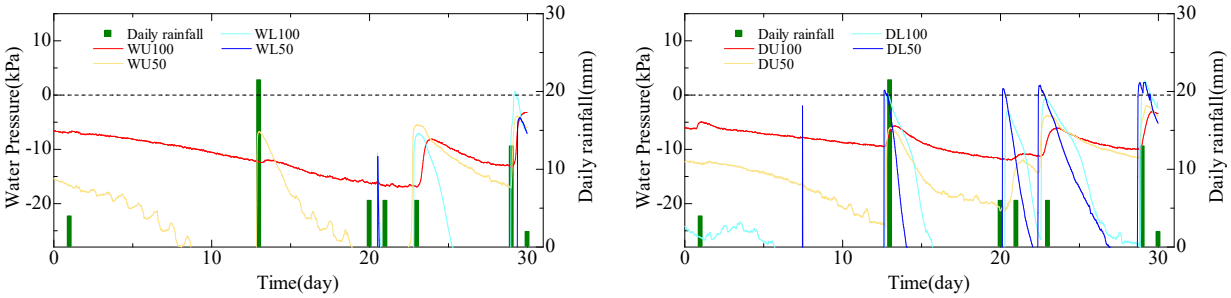

(a) Wet side (b) Dry side

Figure 5: Monitored water pressure (November, 2022)

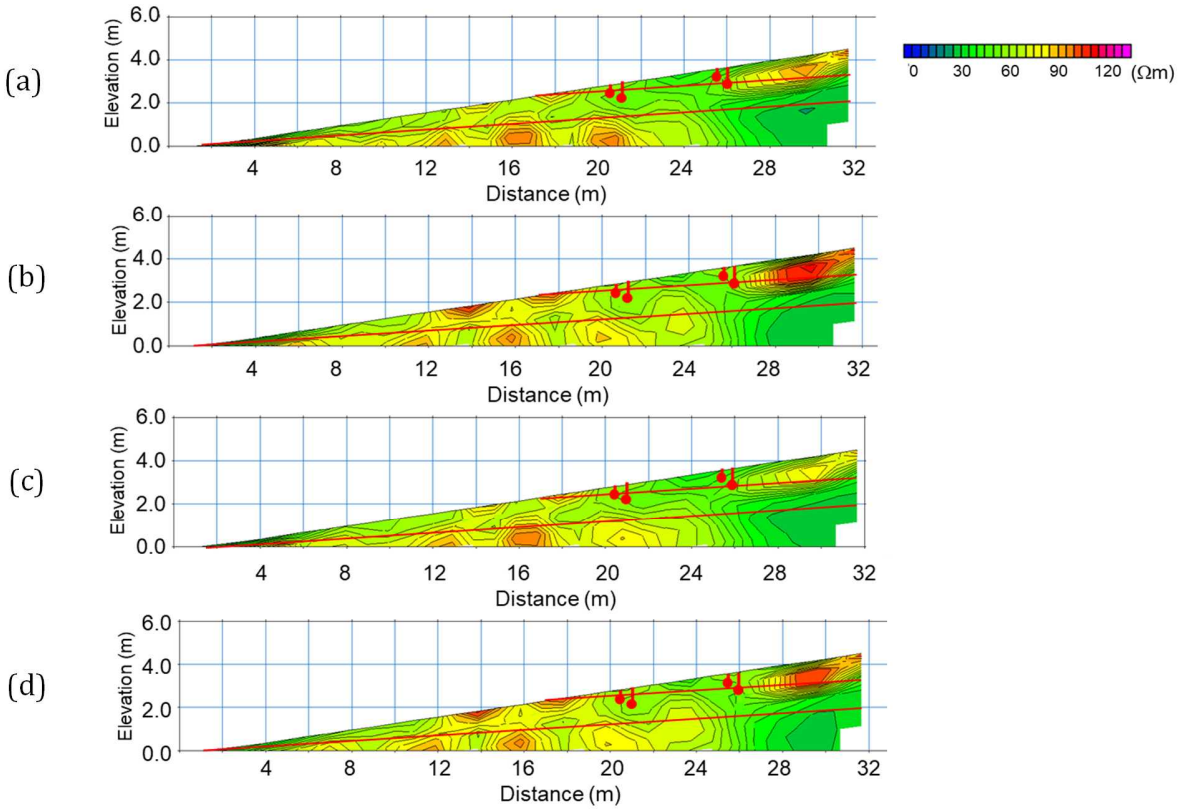

Figure 6: Distribution of electrical resistibility; (a) Wet side on November 21st, (b) Dry side on November 21st, (c) Wet side on November 25th, (d) Dry side on November

prospecting were placed at about 100 cm intervals on the slope surface. Figure 5 shows the fluctuation in water pressure as monitored by tensiometers in November of 2022. These measurements determined that water pressure increased with rainfall and gradually decreased after rainfall ended. In these results, measured positive water pressure signifies that perched water has formed at the given depth. Monitoring data indicates that perched water formed for short periods of time under rainfall only on the Dry side. The tensiometers on the Dry side are more sensitive to rainfall and showed quicker dissipation, indicating a higher permeability coefficient despite the Wet and Dry side layers being constructed to the same degree of compaction. Figure 6 shows electrical resistibility distribution by electrical prospecting

conducted on November 21st and 25th. The electrical prospecting directly measures the apparent electrical resistibility, which is the average resistibility between electrodes. Therefore, to determine the true electrical resistibility distribution, it is necessary to perform a spatial inversion analysis that considers the electrode spacing and geometric form of the ground surface. Figure 6 was obtained through the spatial inversion analysis. In these figures, the borders between Layers a and b and between Layers b and c are expressed by red lines, and locations of tensiometers are expressed by red circles. Lower electrical resistibility (expressed by bluer area in the figure) indicates higher water content. Regions with clearly low electrical resistibility were not observed in these results, indicating that neither perched water nor a phreatic surface formed. During the 2022 observation, hardly significant rainfall after the embankment's completion, in addition to the slope of the perched aquifer, caused the perched water to disappear faster than expected. The soil moisture meters used in this experiment convert the dielectric constant of the soil into a moisture content value. However, its resolution decreases as it approaches a saturated state. As the embankment was compacted with a saturation level of 0.8 or higher during construction, it was likely difficult to capture increases in saturation due to rainfall. Therefore, to observe perched water in such an embankment, a tensiometer can be considered more effective than a moisture meter. In addition to natural rainfall, a sprinkler test was conducted on July 5th and 6th of 2023. Water was applied to the upper half of the slope twice a day using a sprinkler truck, simulating a total rainfall equivalent of 20 mm over approximately 10 minutes at each application. Electrical resistibility surveys were conducted before, between, and after the watering events to examine the subsurface moisture distribution during the formation and dissipation of perched water. For higher resolution moisture content distribution, the spacing between electrodes was halved, and measurements were conducted only at the upper half of the slope.

Experimental results of the sprinkler test

Figure 7 shows changes in water pressures obtained from the tensiometers during the sprinkler test. The zero point on the horizontal axis represents 9:30 a.m. on July 5th, and measurements were taken for 30 hours until 3:30 p.m. the following day. It rained during the morning of July 5th, followed by heavier rain from late afternoon into the night. The orange broken lines in the figure represent the times when electrical prospecting was conducted, and prospecting data is classified using circled numbers at the top of the figure. The blue arrows denote the timing of the sprinkler water. Tensiometers WL100 and DU100 are not displayed here because they were damaged due to long-term monitoring. Before conducting the sprinkler test (0→1hour), it was confirmed that there was no perched water at the tensiometer installation positions on either the Wet side or the Dry side. Subsequently, after the first sprinkler application (4→5hour), perched water formed at deeper locations (WU100, DL100). The delayed increase in water pressure observed in the shallow tensiometers suggests that the perched water, formed at deeper locations, developed over time following the sprinkler test. However, the shallow tensiometers on the lower side of the slope indicate an earlier rise in water pressure than those on the upper side of the slope. This is likely due to the inclination of the aquifer, which causes soil water to move downward within the embankment. Due to a certain amount of natural

rainfall during the night of July 5th, the water pressure remained high. On the Dry side, further development of perched water was observed following the sprinkler test conducted the next day (23→25 hour). As previously mentioned, the Dry side shows more sensitivity to rainfall. In the case of the water sprinkler test, temporal changes were expected between each survey result due to the short survey intervals. Therefore, in addition to conventional inversion analysis for electrical prospecting (spatial distribution of resistibility), time-lapse analysis was also conducted to account for changes in resistibility over time. Figure 8 shows the electrical resistibility distribution before the sprinkler test, as obtained through spatial inversion analysis. During the sprinkler test, a combination of time-lapse and spatial inversion analysis was conducted by performing electrical prospecting at regular intervals in time along the same surve y line. This allowed for the reduction of the impact of localized anomalies by considering

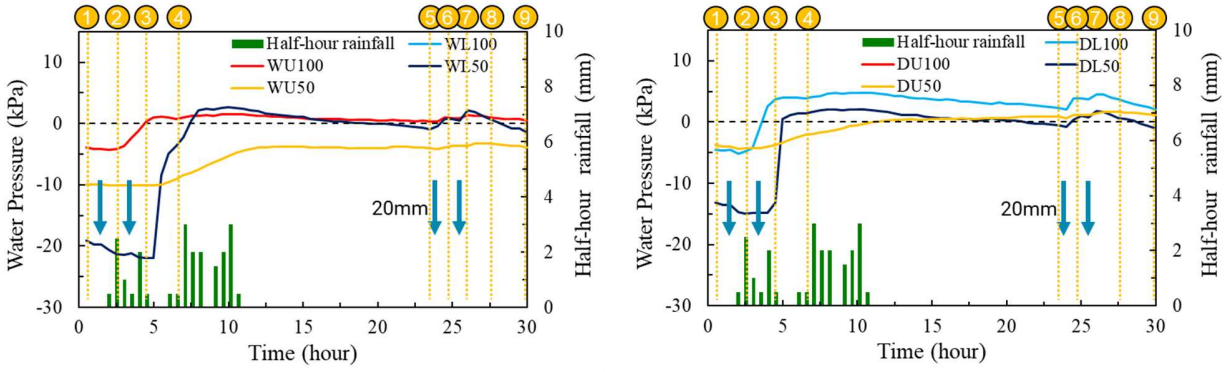

(a) Wet side (b) Dry side

Figure 7: Monitored water pressure (sprinkler test)

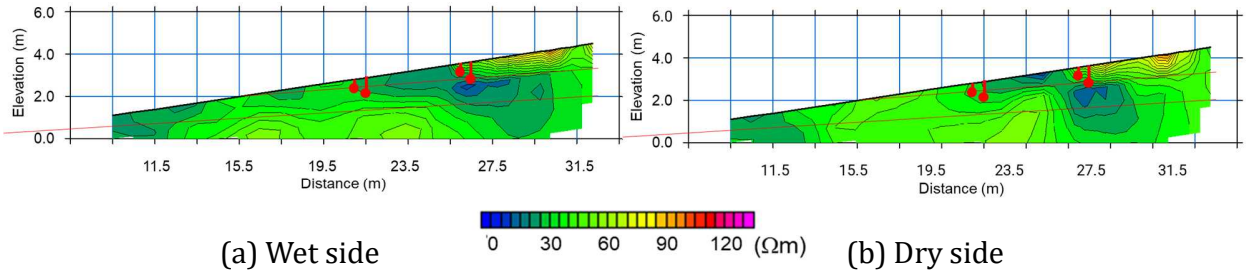

(a) Wet side (b) Dry side

Figure 8: Distribution of electrical resistibility at prospecting ① by spatial inversion analysis

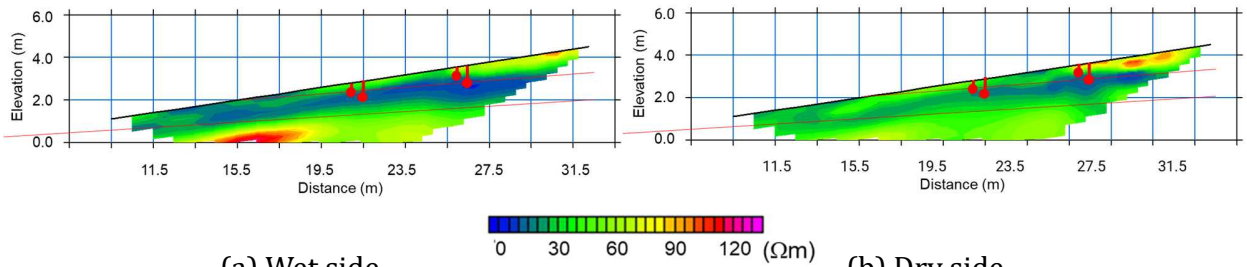

(a) Wet side (b) Dry side

Figure 9: Distribution of electrical resistibility at prospecting ① by combination of time-laps and spatial inversion analysis

the differences in temporal changes. Figure 9 shows the electrical resistibility distribution before the sprinkler test, obtained through time-lapse inversion analysis. In this figure, a low electrical resistibility region, which indicates a high moisture content on the perched aquifer, Layer b, can be clearly observed. This is likely because a perched water layer of a certain thickness formed, although it did not reach the depth of the tensiometer installation before the sprinkler test. Figure 10 shows the changing rates of resistibility distribution determined from the prospecting results ① (shown in Figure 9). As indicated in Figure 7, on the first day of the sprinkler test, the high intensity of the sprinkler application seemed to suppress infiltration

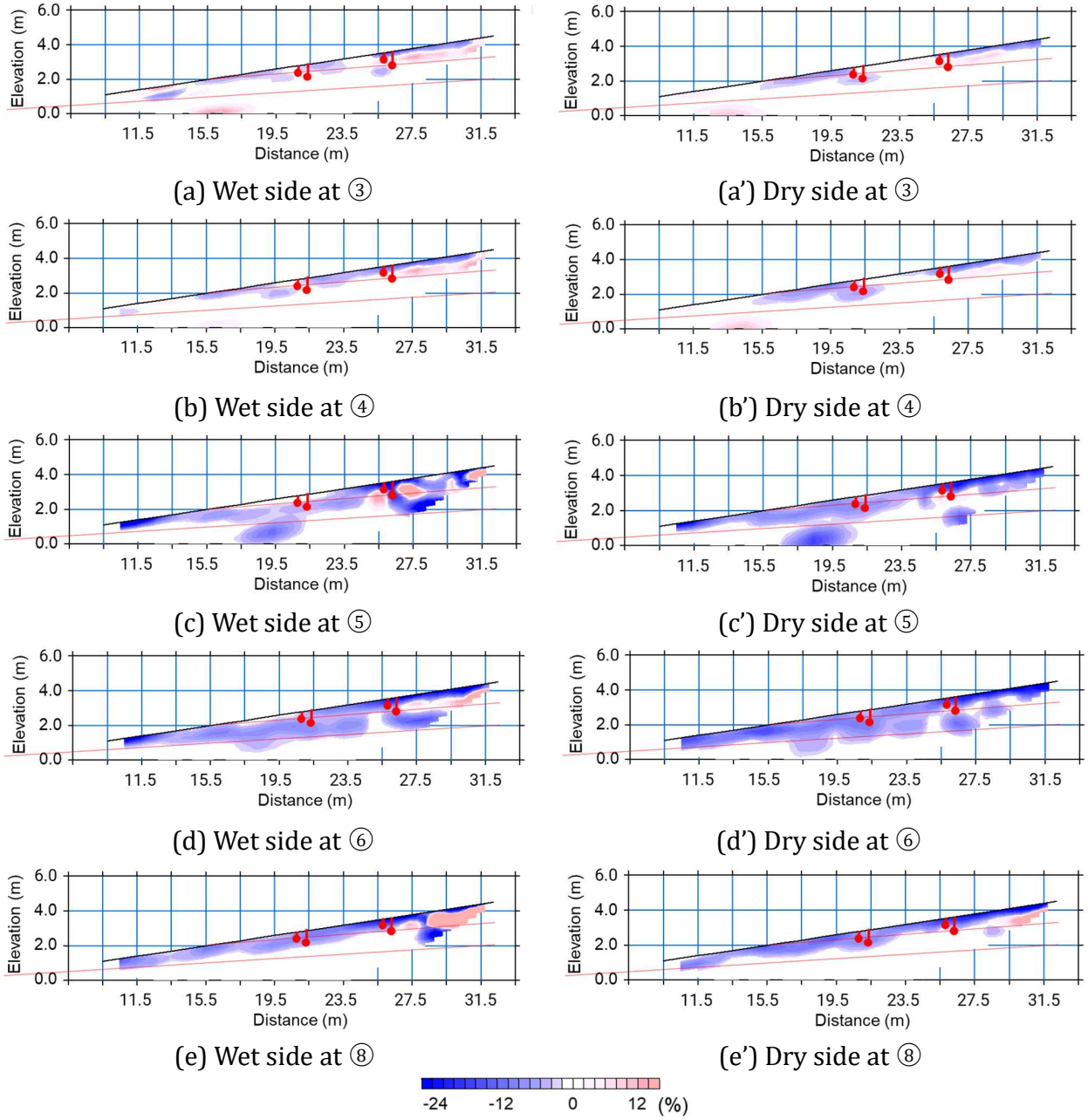

(a) Wet side at ③ (a') Dry side at ③

(b) Wet side at ④ (b') Dry side at ④

(c) Wet side at ⑤ (c') Dry side at ⑤

(d) Wet side at ⑥ (d') Dry side at ⑥

(e) Wet side at ⑧ (e') Dry side at ⑧

Figure 10: Distribution of differential electrical resistibility from ①

from the surface, and water pressure measured by the tensiometers continued to rise even at the final survey time, indicating that perched water was still forming. Consequently, the electrical resistibility prospecting only detected a decrease in resistibility in Layer a. By the morning of the following day (prospecting ⑤), the region of decreased resistibility expanded to Layer b, suggesting the formation of perched water. The higher permeability coefficient on the Dry side appears to allow relatively faster water flow toward the slope toe (prospecting ⑥). Additionally, the measurement conducted after the sprinkler test (prospecting ⑧) confirmed the dissipation of the perched water.

Numerical simulation

To simulate the formation and dissipation processes of perched water in embankments, a rainfall infiltration simulation was conducted using the soil/water/air coupled finite element analysis code DACSAR-MP [2], which allows for detailed saturated-unsaturated seepage analysis. In this study, the analysis area was set above Layer c (Figure 11). The lower and right boundaries of the analysis area were set as undrained boundaries, while a constant pressure head of 0 m was applied only to the toe area, and a flow boundary corresponding to rainfall intensity was applied to the slope surface. The permeability of each layer was determined from Figure 7. Table 1 summarizes the input material parameters for the embankment soil, and Figure 12 shows its soil-water characteristic curve. Rainfall intensities of 5 mm/h, 10 mm/h, and 20 mm/h were applied to achieve a total rainfall of 60 mm in each case, and a resting period of 7 days after rainfall was provided to clarify the rainfall conditions under which perched water forms and dissipates.

Figure 11 shows the distribution of the degree of saturation obtained from rainfall simulations of 5 mm/h and 20 mm/h rainfall intensity. Immediately after rainfall ((a) and (a')), perched

Table 1: Input material parameters

Layer	λ	κ	M	n_E	a	n_s	m	k_w (m/day)	k_a (m/day)
a	0.087	0.009	1.375	1.0	10.0	1.0	0.6	8.64	864
b								0.259	25.9

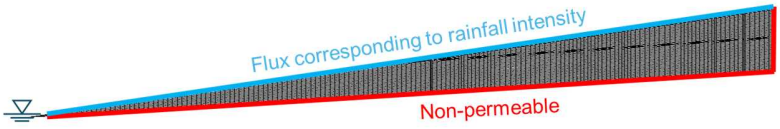

Figure 11: Analytical area and boundary conditions

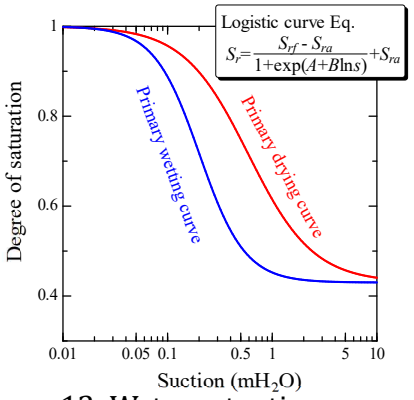

Figure 12: Water retention curves

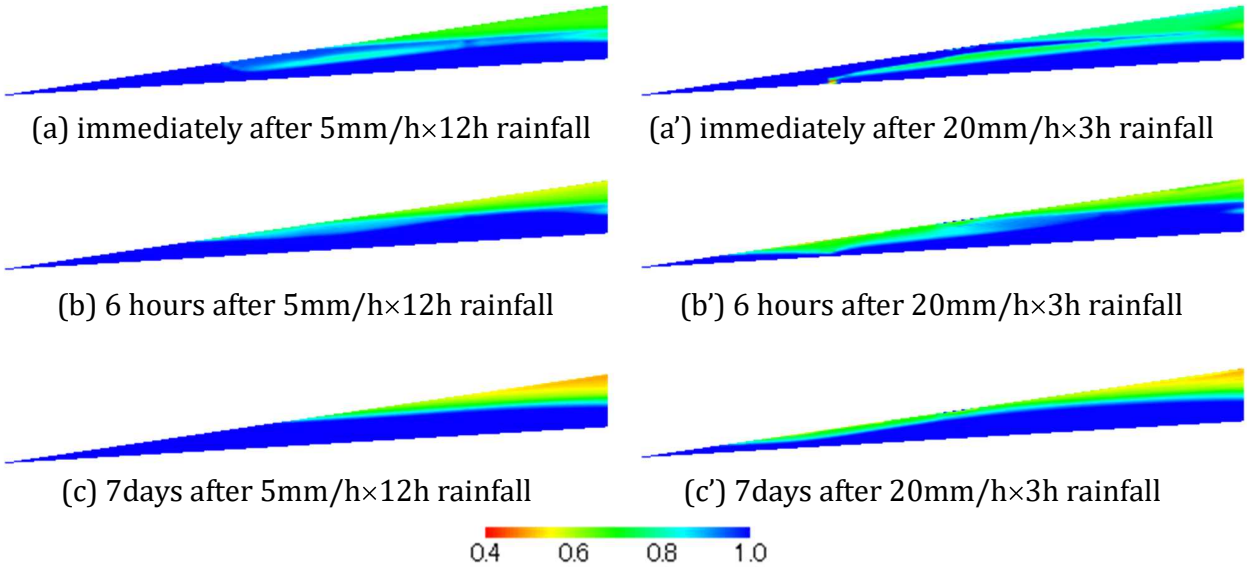

(a) immediately after 5mm/h×12h rainfall (a') immediately after 20mm/h×3h rainfall

(b) 6 hours after 5mm/h×12h rainfall (b') 6 hours after 20mm/h×3h rainfall

(c) 7days after 5mm/h×12h rainfall (c') 7days after 20mm/h×3h rainfall

Figure 11: Distribution of degree of saturation obtained from rainfall simulation

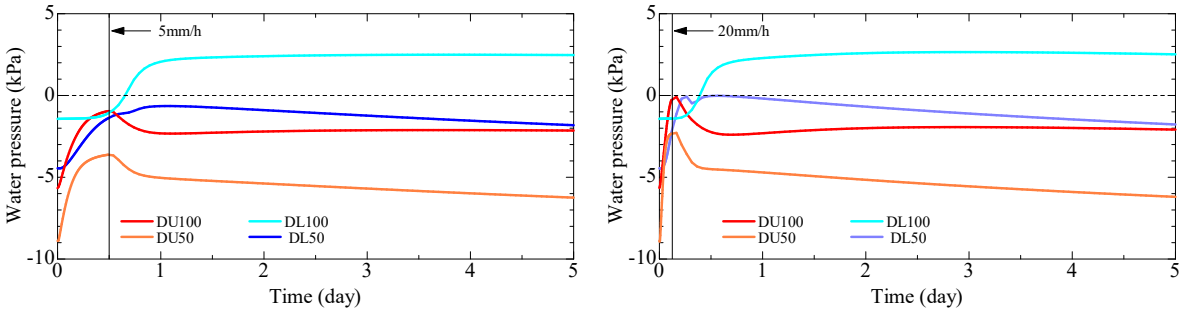

(a) 5mm/h × 12h (b) 20mm/h × 3h

Figure 12: Fluctuation in water pressure within embankment

water formed at Layer a in both cases. However, in the case of (a) with lower rainfall intensity, downward flow into the lower Layer b progressed, resulting in a thinner perched water in Layer a. After 6 hours of rest following rainfall, the perched water in Layer a became continuous with the perched water in Layer b and discharged from the toe of the embankment over time. Here, higher rainfall intensity resulted in a higher phreatic surface in the upper part of the embankment. These results clearly demonstrate that, as observed in the electrical prospecting conducted shortly after rainfall during sprinkler tests, perched water can be temporarily detected in Layer a. However, in electrical prospecting conducted several days later, perched water appeared to be present only in Layer b. This indicates that in cases like this experimental model, where layers with different permeability coefficients are inclined, perched water tends to disappear relatively quickly. In actual construction, loose compaction using compaction machinery was difficult to achieve. In actual model embankment construction, Layer a was more tightly compacted than the designed compaction degree of 85%, which makes the formation of perched water in Layer a even less apparent. To compare the temporal changes in the thickness

of perched water formed in Layer b, Figure 12 shows the pore water pressure changes at the tensiometer installation locations shown in Figure 4. Regardless of rainfall intensity, water pressure decreased at the tensiometer location on the upper slope (DU) after rainfall. In contrast, at the tensiometer location on the mid-slope (DL), water pressure increased after rainfall due to inflow from the upper slope. On the upper slope, under high rainfall intensity, the vertical downward flow of infiltrating water near the slope surface caused an increase in water pressure for a certain period even after the rainfall ended. This difference in the movement behavior of infiltrating water manifests as variations in the formation and dissipation trends of perched water depending on rainfall intensity.

Conclusions

Water movement monitoring within a model embankment with differing soil layers, alongside numerical simulation, was conducted to investigate the mechanisms of perched water formation and dissipation. Consequently, the following conclusions were obtained.

(1) Differences in the degree of compaction can lead to the formation of perched water, even with the same soil materials.

(2) While the formation of perched water is easily facilitated by rainfall infiltration, its disappearance requires time. However, when the perched water-forming layer is inclined, perched water formed by rainfall disappears relatively quickly.

(3) The trends in perched water formation and dissipation vary depending on rainfall intensity. Additionally, they are expected to be influenced by factors such as preceding rainfall and the duration of rainfall. Therefore, monitoring with tensiometers and electrical prospecting are considered effective tools for embankment management.

References

[1] R. Fukada, Y. Higo, Y. Ohtake, Y. Nanno and R. Kato. Production of heterogeneous spatial distribution of hydraulic conductivity for embankments and its application to unsaturated seepage analysis under rainfall condition. Journal of JSCE A2 (Application Mechanics), 73(2): I_791-I_799, 2017 (in Japanese).

[2] Y. Sugiyama, K. Kawai and A. Iizuka. Effects of stress conditions on B-value measurement. Soils and Foundations, 56(5): 848-860, 2016.